Investigation of corrosion inhibition and adsorption properties of Pyridine-2-aldehyde nicotinic hydrazone for mild steel in HCl solution.

Authors: Dharmendra Kumar Singh[a] *

Affiliation: P. K. Roy Memorial College, Dhanbad, Jharkhand, India.

ABSTRACT

Schiff's base of Pyridine 2-Aldehyde namely N'-(Pyridine-2-ylmethylene) nicotinic hydrazone was synthesized. The corrosion inhibition and adsorption properties for mild steel in 1M HCl solution were investigated using Electrochemical, weight loss measurements and quantum chemical calculation method. Adsorption of inhibitor on mild steel surface follows Langmuir adsorption isotherm with physisorption mechanism. Potentiodynamic study indicates that it acts as mixed type inhibitor. It exhibits inhibition efficiency of 94.7% at 2 mM concentration. All the theoretical and experimental results are in good agreement.

Keywords: Mild steel, Polarization, EIS, Corrosion Inhibitor, Acid corrosion, DFT.

1. Introduction

Corrosion of mild steel results into huge economic loss worldwide, because of its sensitivity towards acid corrosion. Hence, prevention and mitigation of corrosion of mild steel especially in acidic media is a matter of concern today for sustainable development **[1-2].** The use of organic compounds as inhibitor is one of the most efficient and cost-effective method to protect metals against acid corrosion. Literature survey reveals that these inhibitors usually adsorb on the metal surface either by physisorption or chemisorption or through both the mechanism and block the active sites on the metal surface **[3-5].** The adsorption of inhibitor molecules produces a protective film on metal surface that reduce the aggressive attack of acid solution, consequently reduces the corrosion extent **[6].** In general**,** organic compounds containing heteroatom like nitrogen, oxygen, sulphur or conjugated Π bonds or >C=N- group or aromatic rings etc. in their structure often show good corrosion inhibition properties for mild steel against acidic media. In addition, the ability of inhibitor towards metal protection also depends upon the chemical composition, geometry, molecular parameters and environment **[7-10].** Nicotinic acid hydrazones are usually non-toxic and possess the various pharmacological properties like anti- inflammatory, analgesic agent and antimicrobial. Various researchers have also been studied as corrosion inhibitor properties of these compounds for mild steel in acidic media where they have been demonstrated good corrosion inhibition ability for mild steel in acid media **[11-12].** The objective of this work was to synthesize Schiff's base using nicotinic acid hydrazide and Pyridine-2-aldehyde and to investigate its corrosion inhibition properties and the mechanism of protection for mild steel in 1 M HCl solution using electrochemical, weight loss and quantum calculations methods. Quantum chemical calculations using DFT method as a theoretical method has extensively been used to investigate correlation between molecular parameters of the inhibitor molecule, adsorption mechanism of the inhibitor molecules on the metal surface

and their corrosion inhibition ability [**13-14].** Hence in the present study, various molecular parameters of the studied inhibitor molecule have also been calculated by means of DFT method.

2. Materials and Methods

2.1. Synthesis of N'-(Pyridine-2- ylmethylene) nicotinic hydrazone

N'-(Pyridine-2-ylmethylene) nicotinic hydrazone was prepared by mixing Pyridine-2-aldehyde with Nicotinic acid hydrazide in ethanol. The reaction mixture was refluxed and then cooled to room temperature **[15].** After cooling, the precipitate was obtained that again recrystallized in ethanol. The chemical structure of the synthesized inhibitor is shown in Fig.1. The structure and purity of the compound has been confirmed by TLC, FT-IR and ^{1}H NMR spectroscopic methods.

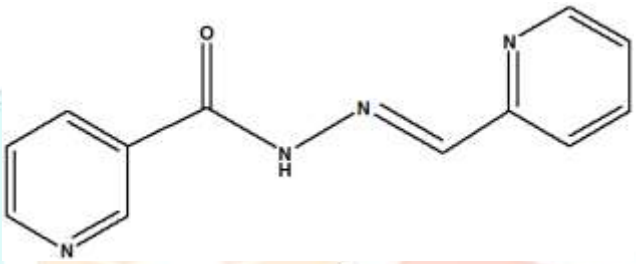

Fig.1. Chemical structure of the synthesized corrosion inhibitor: N'-(Pyridine-2-ylmethylene) nicotinic hydrazone (PYNH).

2.2. Material and sample preparation

In this study, mild steel having chemical composition (wt%): C- 0.07, Mn-0.42, P-0.029, S-0.014, Al-0.041 and rest Fe was used for corrosion test. The working electrode for electrochemical study, which is mild steel, was embedded in epoxy resin in such a way that only cross-sectional area of 1 cm^2 could make contact with test solution. Before each experiment the exposed mild steel surface was abraded with abrasive papers (grade 320 to 1200), then rinsed with double distilled water and dried with cool air. Analytical grade 37% HCl solution was used to prepare the test solution (1 M HCl) using double distilled water. The concentrations of the corrosion inhibitor were kept in the range of 0.25 to 4.00 mM.

2.3. Electrochemical measurements

Before each electrochemical test, the working electrode was immersed in the test solution till to attain steady-state open circuit potential (OCP). The electrochemical impedance measurements were carried out at the steady state over a frequency range of 100 kHz - 0.1Hz with 5mV peak-to-peak amplitude using the AC signal. The obtained experimental data were fitted to suitable equivalent circuit diagram and important impedance parameters were calculated. The percentage inhibition efficiency of the studied inhibitor was calculated using the following equation [11]:

$$\eta\% = \frac{R_P - R_P^0}{R_P} \times 100\% \qquad (1)$$

Where R_p and R_P^0 are the polarization resistance in the presence and absence of inhibitor, respectively.

The potentiodynamic polarization measurements were carried out in the potential range -250 to +250 mV relative to the OCP at a scan rate of 1 mVs^{-1}. Platinum rod was used as counter electrode, saturated calomel electrode (SCE) as the reference electrode and mild steel as working electrode. The electrochemical parameters like corrosion current density (i_{corr}), corrosion potential (E_{corr}), cathodic and anodic Tafel slopes (β_c and β_a) were derived from polarization curves by extrapolation method. The inhibition efficiency (η %) of the inhibitor was determined by using the following relationship [16]:

$$\eta\% = \frac{i_{corr}^0 - i_{corr}}{i_{corr}^0} \times 100 \qquad (2)$$

Where i_{corr}^0 and i_{corr} are the corrosion current density in the absence and presence of the inhibitor respectively.

Electrochemical measurements were carried out using CHI 660C Electrochemical Workstation at 30 ˚C in a three-electrodes assembly in stagnant condition.

2.4. *Weight loss measurements*

Mild steel specimens in triplicate were immersed in 1 M HCl for 3 hrs. at 30 ˚C in the absence and presence of various concentrations of the inhibitor. The mass of each mild steel specimen was determined before and after immersion and the average of the triplicate measurements was used. The corrosion rate (C_R) and the percentage inhibition efficiency (η %) were determined by the following equations:

$$C_R = \frac{\Delta W}{S \times t} \qquad (3)$$

Where Δw is the weight loss after corrosion, 'S' is the total exposed surface area of the specimen, 't' is time of exposure.

$$\eta\% = \frac{C_R^0 - C_R}{C_R^0} \times 100 \qquad (4)$$

Where $(C_R)_0$ and $(C_R)_{ii}$ are the corrosion rates in the absence and presence of inhibitor.

2.5. Adsorption isotherm:

As most of the corrosion inhibitor protect metal surface in acidic environment by adsorbing on the surface of metal and blocking the active sites. In order to comprehend the interaction between the inhibitor molecules at the mild /solution interface, the various isotherms like Freundlich, Temkin and Langmuir isotherms were examined from the data obtained from potentiodynamic polarization measurements.

2.6. Quantum chemical calculations

Quantum chemical calculations were performed with complete geometry optimization using density functional theory (DFT) method at B3LYP/6-31++G(d,p) level as implemented in Gaussian 09W software. The important molecular parameters like E_{HOMO}, E_{LUMO} and dipole moment (μ) for the neutral inhibitor

molecule were calculated.

3. Results and discussion

3.1. *Conformation of structure of synthesized inhibitor*

3.1.1. *FT-IR spectra*

FT-IR spectra of the synthesized inhibitor showed the following absorption bands:

For PYNH: I.R (KBr cm^{-1}); 3560, 3396, 3199, 3029, 1661, 1592, 1563, 1292, 1152, 923, 722, 622.

In FT-IR spectra, the absorption bands at 1592 cm^{-1} (PYNH) confirmed the presence of -C= N- group (Schiff's base) in the synthesized inhibitor.

3.1.2. ^{1}H NMR spectra

^{1}H NMR spectra showed the following peaks **[Fig. 2]:**

For PYNH: ^{1}H NMR (δ ppm, DMSO); 7.39-7.42 (t,1H, PyH), 7.54-7.57(t, 1H, PyH), 7.84-7.89(t, 1H, PyH), 8.00-8.02(d, 1H, PyH), 8.26-8.29(d, 1H, PyH), 8.47(s, 1H, N=CH), 8.60-8.61(d, 1H, PyH), 8.76-8.77(d, 1H, PyH), 9.10(s, 1H, PyH), 12.23(s, 1H, NH-CO-).

The data of ^{1}H NMR spectra confirmed the expected hydrogen distribution in the synthesized PYNH.

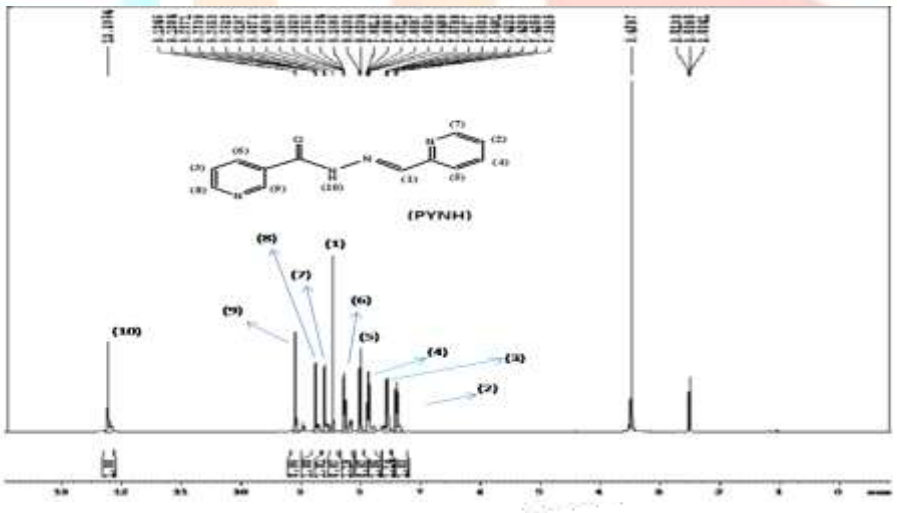

Fig.2. ^{1}H NMR Spectra of PYNH

3.2. Potentiodynamic polarization measurements

The potentiodynamic polarization curves for mild steel in the absence and presence of different concentrations of the inhibitor PYNH are illustrated in **Fig. 3**. From these figures, it is obvious that the addition of inhibitor does not change the nature of potential vs. current density curves but it significantly decreases both cathodic as well as anodic branch of the curves towards lower current density with respect to blank solution. In addition, it can be seen from **Fig. 3** that the magnitude of shifting of cathodic branch towards lower current density is comparatively more than anodic branch of polarization curves. It suggests that these compounds have potential to suppress both cathodic as well as anodic reaction on metal surface; consequently, they can be classified as mixed type inhibitor with predominating in cathodic nature.

Furthermore, the cathodic branch of polarization curves give rise to almost parallel lines. It indicates that the addition of PYNH inhibitor to acidic solution does not amend mechanism of cathodic hydrogen evolution process or reduction of H^+ ion on metal surface; consequently, corrosion may be kinetic controlled.

The electrochemical parameters like corrosion current density ($i$corr), corrosion potential (Ecorr), cathodic and anodic Tafel slopes (βc and βa) derived from polarization curves by extrapolation method as well as the percentage inhibition efficiency are illustrated in **Table 1**. From this table, it is evident that on addition of inhibitor PYNH to acid solution extensively brings down the value of corrosion current density with respect to that of blank solution (acid solution without inhibitor). In addition, as the concentration of inhibitor increases, the value of corrosion current density ($i$corr) gradually decreases and at higher concentration it becomes almost impossible to differentiate. It can be attributed to the formation of protective film by adsorption of inhibitor molecules at metal /solution interface that blocks both cathodic and anodic sites and reduces the attack of aggressive acid solution on metal surface **[16-18].** On increasing inhibitor concentration, surface coverage on metal surface increases which results into decrease in corrosion current density. Furthermore, it can be seen from **Table 1** that the value of Ecorr in the presence of inhibitor PYNH, deviates from that obtained in the absence of inhibitor but this shift is not more than 85 mV with respect to blank solution**.** Literature survey reveals that any inhibitor can be classified as cathodic or anodic if shift in corrosion potential in the presence of inhibitor in acid solution is more than 85 mV with respect to acid solution in the absence of inhibitor **[19-20]**. On this basis, the studied inhibitor may be classified as mixed type inhibitor with predominance in cathodic behavior. The obtained value of percentage inhibition efficiency of PYNH at higher concentration at 4 mM is 94.1% indicates that it is an efficient corrosion inhibitor for mild steel in acid solution.

Table 1 Electrochemical polarization parameters for mild steel in 1 M HCl solution in the absence and presence inhibitor PYNH at 30˚C.

Inhibitor	Conc (mM)	$-E$corr (mV vs SCE)	$-\beta$c (mV dec $^{-1}$)	Ba (mV dec $^{-1}$)	$i$corr (mA cm^{-2})	θ	η %
Blank		470	146.6	85.2	1.53		
PYNH	0.25	521	115.3	82.6	0.36	0.76	76.1
	0.50	529	122.6	88.0	0.35	0.76	77.2
	1.00	519	115.4	85.0	0.12	0.92	92.2
	2.00	511	128.3	81.9	0.08	0.95	94.7
	4.00	532	114.3	96.2	0.09	0.95	94.1

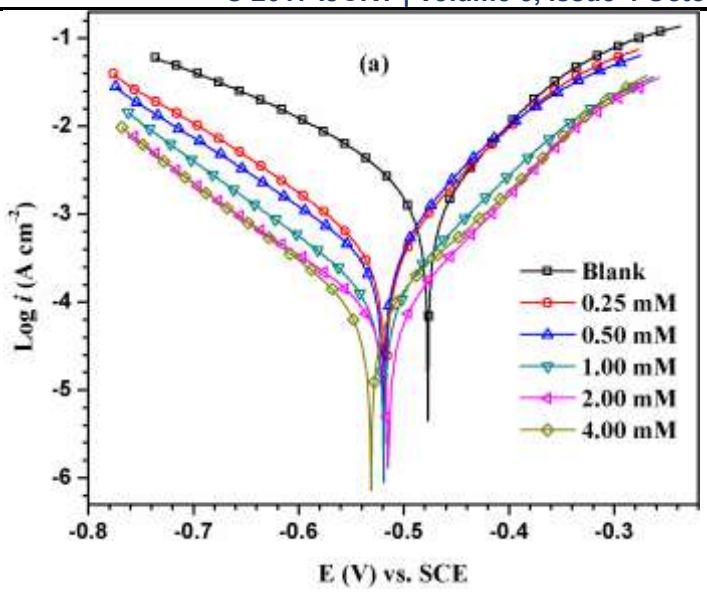

Fig.3. Polarization curves for mild steel in 1 M HCl in the presence and absence of inhibitor PYNH at 30˚C.

3.3. Electrochemical impedance spectroscopy (EIS)

The Nyquist plots of mild steel in 1 M HCl solution in the absence and presence of different concentrations of PYNH are represented in **Fig. 5**. It can be seen that all the Nyquist plots exhibit single depressed capacitive loop with one time constant in Bode plot Fig. **6**. It suggests that the corrosion of mild steel in 1 M HCl is mostly controlled by charge transfer process and usually related to the double layer behavior. The deviation/depression in semicircle can be related to non-ideal electrochemical capacitive behavior at metal/ solution interface. Such phenomenon is called dispersing effect which is often attributed to the surface roughness, chemical inhomogeneities, the adsorption of inhibitor molecules and the degree of polycrystallinity **[21-22].** Furthermore, the diameter of the capacitive loops increases appreciably with increasing inhibitor concentration. It may be owing to increase of surface coverage of inhibitive molecules on mild steel surface **[23].** To determine electrochemical impedance parameters, experimental EIS data were fitted to equivalent circuit models as shown in **Fig. 4a & 4b.** In the absence of inhibitor, equivalent circuit model of **Fig. 4a** fits well our experimental data (solid line represents fitted results). In this equivalent circuit, R_S is the solution resistance, R_{Ct} denotes the charge transfer resistance and CPE is the constant phase element. The CPE is used in the circuit instead of pure double layer capacitor in order to take into account the heterogeneity of electrode surface resulting from surface roughness, impurities, grain boundaries, adsorption of inhibitor, and formation of porous layer **[24].** The CPE is composed of a component Y_0 and a coefficient n, which can be represented by the expression **[25]:**

$$Z\text{CPE} = Y_0^{-1}(j\omega)^{-n} \qquad (5)$$

Where Y_0 is a proportional factor; ω is angular frequency, j is imaginary number ($j^2 = -1$), n is a deviation parameter or phase shift ($-1 \leq n \leq +1$), which quantify the deviation from the ideal capacitive behavior.

In the presence of inhibitor, equivalent circuit model of **Fig. 4b** fits well our experimental EIS data as represented in **Fig. 5** (solid lines represent fitted results). The addition of inhibitor to 1 M HCl solution has significantly changed the impedance response of mild steel. In the presence of inhibitor, Nyquist plots displayed a depressed capacitive loop (larger) at high frequency region. The capacitive loop (the larger) is

attributed to the charge transfer resistance (Rct), which could correspond to resistance between the metal and outer Helmholtz plane and other one (the smaller) can be related to the adsorption film resistance (Rf), which could correspond to adsorption of inhibitor molecules on metal surface and/or all other accumulated kinds like corrosion products, inhibitor molecules etc at metal/solution interface **[26-27].** Hence, the contribution of all the resistance correspond to the metal/ solution interface must be taken into account. In the evaluation of Nyquist plots, the difference in real impedance at lower and higher frequencies is commonly considered as charge transfer resistance; while in the present study, this difference is considered as the polarisation resistance (Rp) instead of charge transfer (Rct). In the absence of inhibitor, polarisation resistance consists of only charge transfer resistance (Rct), while in the presence of inhibitor, the sum of Rct and Rf is equivalent to Rp **[28].**

The impedance parameters obtained by fitting EIS data to the equivalent circuits are shown in **Table 2**. On analysing **Table 2**, it is obvious that the value of Rp increases with increasing concentration of PYNH; consequently, inhibition efficiency increases. This can be attributed to the formation of protective film on metal solution interface on addition of inhibitor to acid solution, which acts as barrier for mass and charge transfer. Furthermore, the CPE values (**Table 2**) decrease with increasing inhibitor concentration. This is probably due to the decreasing local dielectric constant and/or an increase in the thickness of electrical double layer **[29-31].**

The Bode plots for mild steel in the presence and absence of different inhibitor concentrations at 30 ˚C are represented in **Fig 6**. From Bode plots, it can be seen that the values of absolute impedance at low frequency increase with increasing inhibitor concentration, which again confirms higher protection of mild steel in 1 M HCl solution with addition of the studied inhibitor. It is attributed to the adsorption of the inhibitor PYNH molecules on mild steel surface in 1 M HCl.

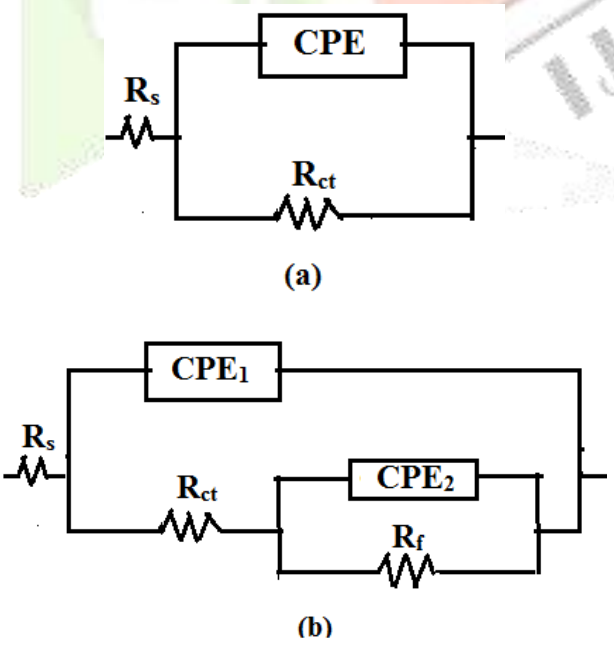

Fig.4. Equivalent circuit diagrams

Table 2

Impedance parameters for mild steel in 1 M HCl solution in the absence and presence of inhibitor PYNH at 30˚C.

Inhibitor	*C* (mM)	*R*s (Ω cm^2)	*R*p (Ω cm^2)	CPE1		CPE2		*η* %
				Y0 ($\mu\Omega^{-1} s^n cm^{-2}$)	*n*1	*Y0* ($\mu\Omega^{-1} s^n cm^{-2}$)	*n*2	
Blank	0.00	0.82	14.5	364.0	0.80		0.00	
PYNH	0.25	0.95	36.4	55.5	0.99	907.5	0.60	60.1
	0.50	1.05	43.3	39.3	0.99	843.3	0.52	66.5
	1.00	0.89	69.0	43.7	0.99	318.6	0.62	79.0
	2.00	1.15	176.1	17.7	0.99	211.6	0.61	91.7
	4.00	0.99	214.5	38.2	0.94	1012.0	0.30	93.4

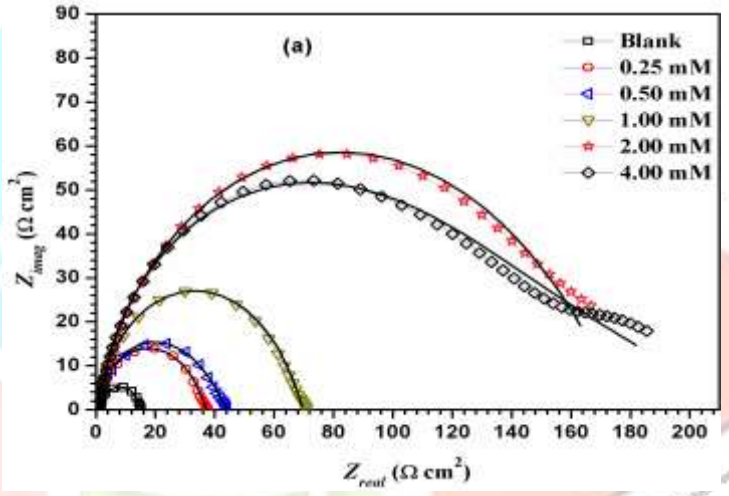

Fig. 5. Nyquist plots of mild steel in 1 M HCl in the absence and presence of different concentrations of inhibitor at 30˚C: (a) PYNH (Solid lines represent fitted results).

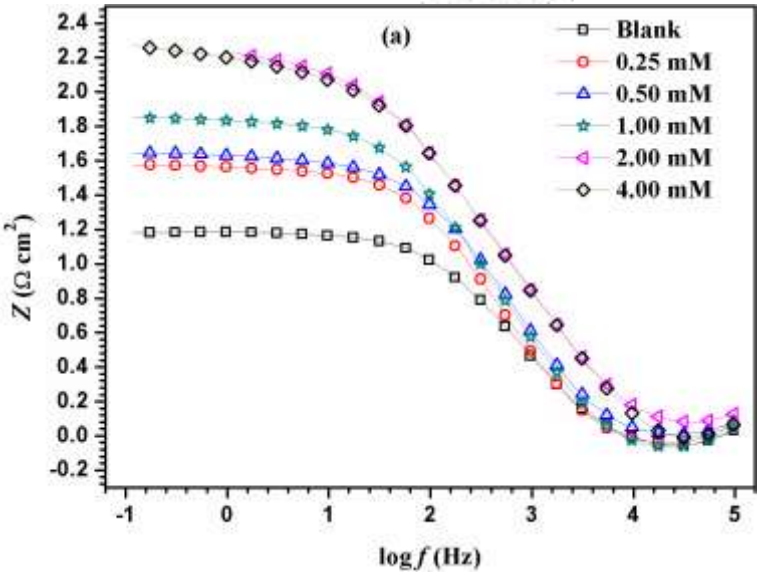

Fig. 6. Bode Plots of mild steel in 1 M HCl solution in the absence and presence of different concentrations of the inhibitor PYNH at 30˚C.

3.4. *Weight loss measurements* and effect of temperature

The variation of corrosion inhibition efficiency (η%) for mild steel in 1 M HCl in the presence of the inhibitor PYNH (at selected inhibitor concentrations of 2 mM and 4 mM) with temperature are illustrated in **Fig.7.** In the presence of 2 mM and 4 mM concentration, the inhibition efficiency of PYNH increases with increasing temperature and shows highest efficiency of 94.69% and 94.87% respectively at 313K then after its efficiency starts to decrease. Such phenomenon implies chemisorption type adsorption of PYNH on mild steel surface. At higher temperature 50 ˚C (323K), lower value of the inhibition efficiency of PYNH may be owing to rapid etching, desorption of the inhibitor, decomposition or rearrangement of the inhibitor **[05]**.

The activation energy (*E*a) and the rate of corrosion (*C*r) of the metal can be represented by the Arrhenius equation as **[26]**:

$$\log C_R = \log A - \frac{E_a}{2.303RT} \qquad (6)$$

Where A is the Arrhenius constant, T is the absolute temperature and R is the gas constant. The activation energy values for the mild steel in the presence and absence of inhibitor are calculated from the slopes of the Arrhenius plots of log *C*r against 1/T as shown in **Fig.8**. The *E*a values in the presence and absence of different concentrations of the inhibitor are shown in **Table.3**. From this table, it is obvious that the values of *E*a in the presence of 2 mM and 4 mM concentrations of PYNH are 43.03 $kJmol^{-1}$ and 49.78 $kJ\ mol^{-1}$ respectively. These values are near about or less than that of uninhibited solution (45.64 $kJ\ mol^{-1}$). This phenomenon can be interpreted as chemisorption tendency predominates in the presence of PYNH. However, it is worth noting that only the value of activation energy for the corrosion of metals can't be the only predictor of types of adsorptions of the inhibitor **[27].**

Table 3

Activation energy for mild steel in 1M HCl in the presence and absence of the inhibitor PYNH.

Inhibitor	Concentration (mM)	*E*a ($kJmol^{-1}$)
PYNH	0.00	45.64
	2.00	43.03
	4.00	49.78

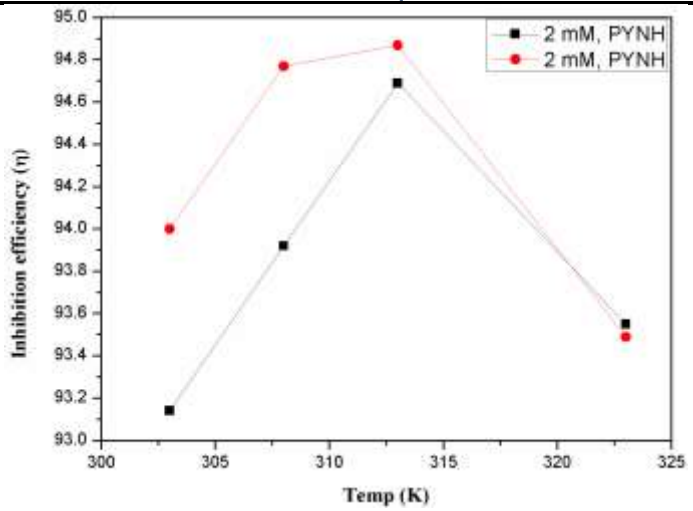

Fig.7. Variation of inhibition efficiency of the inhibitor PYNH with temperature for mild steel in 1 M HCl.

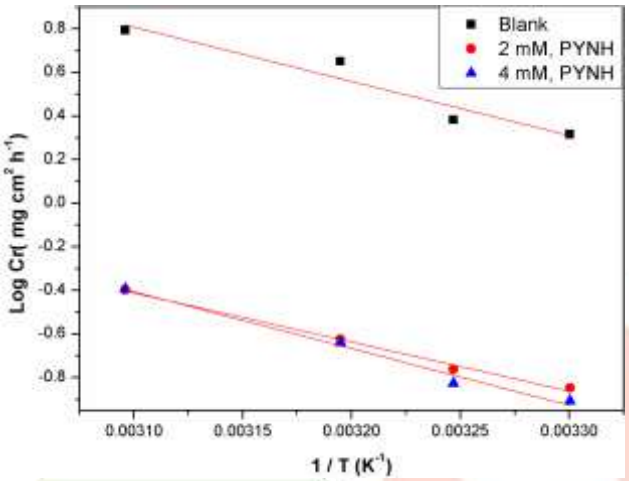

Fig.8. Arrhenius plots of Log *C*r vs. 1/T for mild steel in 1 M HCl in the presence and absence of different concentrations (2.00 mM & 4.00 mM) of the inhibitor PYNH.

3.5. Adsorption Isotherm

The adsorption isotherm can provide essential information about the insight into the adsorption of the inhibitor at mild/solution interface. Keeping this in view, the experimental data (**Table.1**) obtained from potentiodynamic polarization measurements at 30°C were fitted to various isotherms like Langmuir, Frumkin and Temkin isotherms. In the presence of inhibitor PYNH, the plots of C/θ vs. C give straight line as shown in **Fig.9.** The linear correlation coefficients (R^2) are close to unity (**Fig.9**) for the inhibitor PYNH indicating that the adsorption of PYNH on mild steel surface obeys Langmuir adsorption isotherm (**Eq. 7**).

$$\frac{C}{\theta} = \frac{1}{K_{ads}} + C \qquad (7)$$

where C, Θ and K_{ads} are the inhibitor concentration, surface coverage and equilibrium adsorption constant respectively. The value of K_{ads} for the inhibitor is calculated from the intercept of the straight line **(Fig.9**) is given in **Table 4**.

The relationship between K_{ads} and the standard free energy of adsorption (ΔG^0_{ads}) can be shown as **[28]:**

$$K_{ads} = \frac{1}{55.5}\exp\left(-\frac{\Delta G^{\circ}_{ads}}{RT}\right) \qquad (8)$$

Where 55.5 is the molar concentration of water in the solution expressed in M (mol L^{-1}), R is the gas constant

(8.314 J $K^{-1}mol^{-1}$) and T is the absolute temperature (K). The value of ΔG^0ads for PYNH lies in the range of 33.63 kJ mol^{-1}. It demonstrates spontaneous and strong adsorption of PYNH on the mild steel surface **[11]**. The adsorption of inhibitor on the metal surface can be classified into physisorption or chemisorption on the basis of the values of ΔG^0ads. Literature survey reveals that the value of - ΔG^0ads near or less than 20 kJ mol^{-1} is associated with physisorption, while those around 40 kJ mol^{-1} or higher is associated with chemisorption adsorption**.** In this study, the calculated value of (- ΔG^0ads) for PYNH indicates that the adsorption mechanism may involve both physisorption and chemisorption **[29-30].**

Table.4.

Thermodynamic parameters obtained from Langmuir adsorption isotherms for PYNH

Inhibitor	Kads(M^{-1})	- ΔG°ads (kJ mol^{-1})
PYNH	11.3×10^3	33.63

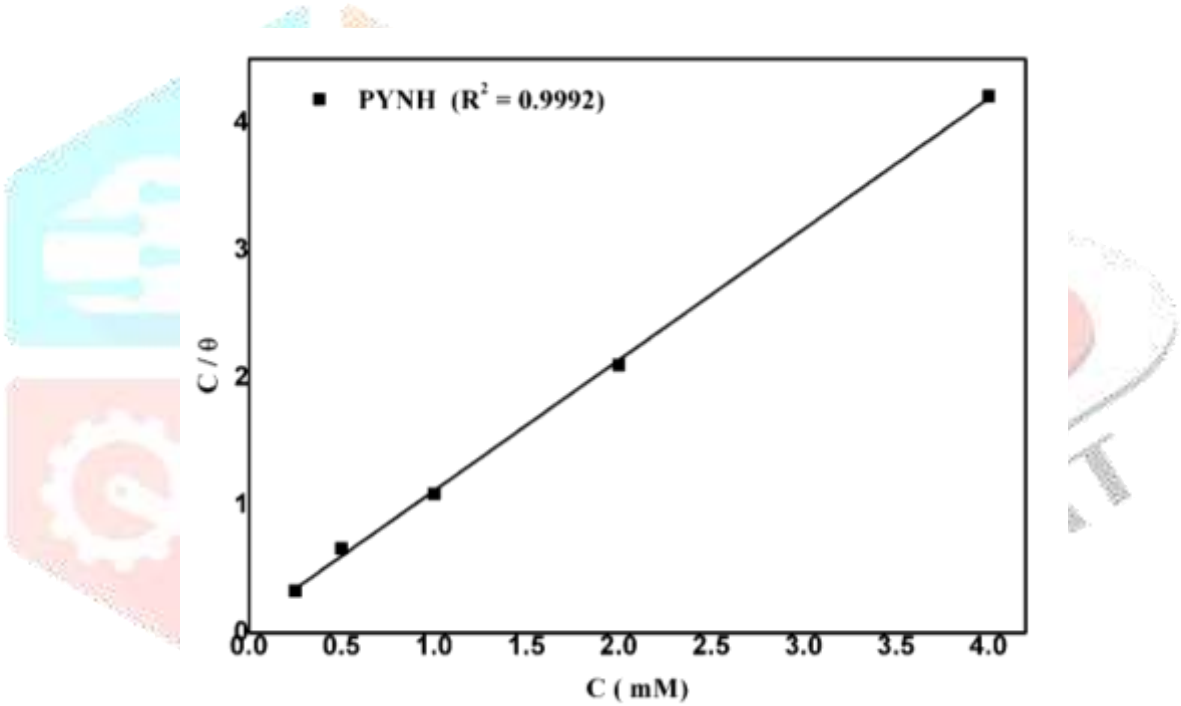

Fig.9. Langmuir adsorption plot for mild steel in1M HCl for PYNH inhibitor at 30˚C

4. Conclusions

(I) The highest inhibition efficiency of inhibitor PYNH is found to be 94.7%. It shows that that PYNH is an efficient corrosion inhibitor for mild steel in 1 M HCl solution.

(II) The inhibition efficiency increases with temp followed by decreases with increase in temperature.

(III) Polarization measurements show that it acts as mixed type inhibitor.

(IV) The adsorption of PYNH on mild steel surface Langmuir adsorption isotherm.

Acknowledgement

D. K. Singh is thankful to University Grant Commission (UGC), ID NO-JVB3-018 for providing financial support.

References

[1] Yan Xie, Yuan Wei Liu, Zhongnian Yang, International Journal of Electrochemical Science, 10, 1292 (2015).

[2] K. R. Ansari, M. A. Quraishi, Ambrish Singh, Journal of Industrial and Engineering Chemistry, 25, 89 (2015).

[3] G. Jit, S.K. Shukla, P. Dwivedi, S. Sundaram, R. Prakash, Journal of Industrial & Engineering Chemistry Research, 50, 11954 (2011).

[4] B. El Mehdi, B. Mernari, M. Traisnel, F. Bentiss, M. Lagrenée, Materials Chemistry and Physics, 77, 489 (2003).

[5] Bin Xu, Wenzhong Yang, Ying Liu, Xiaoshuang Yin, Weinan Gong, Yizhong Chen, Corrosion Science, 78, 260 (2014).

[6] E.E. Ebenso, I.B. Obot, International Journal of Electrochemical Science, 5, 2012 (2010).

[7] Djamel Daoud, Tahar Douadi, Hanane Hamani, Salah Chafaa, Mousa Al- Noaimi, Corrosion Science, 94, 21 (2015).

[8] I.B. Obot, S.A Umoren, Z.M. Gasem, Rami Suleiman, Bassam El Ali, Industrial & Engineering Chemistry Research, 21, 1328 (2015).

[9] E. E. Ebenso, M.M. Kabanda, L.C. Murulana, A.K. Singh, S.K. Shukla, Industrial & Engineering Chemistry Research, 51 12940 (2012).

[10] X. Li, S. Deng, Hui. Fu, Corrosion Science, 53, 324 (2011).

[11] D. K. Singh, M. K. Singh, Asian Journal of Chemistry, 32, 3097 (2020).

[12] D. K. Singh, S. Kumar, G. Udayabhanu, R. P. John, Journal of Molecular Liquids, 216 738(2016).

[13] A. Kosari, M.H. Moayed, A. Davoodi, R. Parvizi, M. Momeni, H. Eshghi, H. Moradi, Corrosion Science, 78, 138 (2014).

[14] I.B. Obot, D. D. Macdonald, Z.M. Zasem, Corrosion Science, 90, 1 (2015).

[15] Ghodrat Mahmoudi, Ali Akbar Khandar, Jan K. Zareba, Michał J. Białek, Masoumeh Servati Gargari, Marjan Abedi, Gotzone Barandika, Donald Van Derveer, Joel Mague, Asad Masoumi, Inorganica Chimica Acta, 429, 1 (2015).

[16] A. S. Fouda, M.A. Ismail, G.Y. EL-Elewady, A.S. Abousalem, Journal of Molecular Liquids, 240, 372 (2017), doi: 10.1016/j.molliq.2017.05.089.

[17] Khaled KF, Electrochemica Acta, 55, 6523 (2010).

[18] C. M. Goulart, A. Esteves-Souza, Carlos Alberto Martinez-Huitle, CiroJosé Ferreira Rodrigues, Maria Aparecida Medeiros Maciel, Aurea Echevarria, Corrosion Science, 67, 281 (2013).

[19] E.S. Ferreira, C. Giancomelli, F.C. Giacomelli, A. Spinelli, Materials Chemistry and Physics, 83, 129 (2004).

[20] Bin Xu, Ying Liu, Xiaoshuang Yin, Wenzhong Yang, Yizhong chen, Corrosion Science. 74, 206

(2013).

[21] V.V. Torres, V.A. Rayol, M. Magalhaes, G.M. Viana, L.C.S. Aguiar, S.P. Machado, H. Orofino, E. D Elia, Corrosion Science, 79, 108 (2014).

[22] T. Paskossy, Journal of Electroanalytical Chemistry, 364, 111 (1994).

[23] Ali A. Abd-Elaal, Ismail Aiad, Samy M. Shaban, Salah M. Tawfik, Atef Sayed, Journal of Surfactants and Detergents,17, 483 (2014).

[24] E. McCafferty, Journal of Electrochemical Society, 119, 146 (1972).

[25] Basak Dogru Mert, Ayse Ongun Yüce, Gülfeza Kardas, Birgül Yazıcı, Corrosion Science, 85, 287 (2014).

[26] I. B. Obot,Eno E. Ebens, Mwadham M. Kabanda, Journal of Environmental Chemical Engineering, 1, 431 (2013).

[27] S. E. Nataraja, T.V.Venkatesha, H.C.Tandon, B.S. Shylesha, Corrosion Science 53, 4109 (2011) .

[28] Lj. Vracar, D.M Drazic, Corrosion Science 44, 1669 (2002).

[29] Shuduan Deng, Xianghong Li, Xiaoguang Xie, Corrosion Science 80, 276 (2014).

[30] Neeraj Kumar Gupta, Chandrabhan Verma, M.A. Quraishi, A.K. Mukherjee, Journal of Molecular Liquids, 215, 47 (2016).